Title

Host- and Helminth-Derived Endocannabinoids That Have Effects on Host Immunity Are Generated during Infection.

Journal

Infection and immunity, 86(11)

ISSN

0019-9567

Authors

Batugedara, Hashini M
Argueta, Donovan
Jang, Jessica C
et al.

Publication Date

2018-11-01

DOI

10.1128/iai.00441-18

Peer reviewed

AMERICAN SOCIETY FOR MICROBIOLOGY | Infection and Immunity®

FUNGAL AND PARASITIC INFECTIONS

Host- and Helminth-Derived Endocannabinoids That Have Effects on Host Immunity Are Generated during Infection

Hashini M. Batugedara,[a] Donovan Argueta,[a] Jessica C. Jang,[a] Dihong Lu,[b] Marissa Macchietto,[c] Jaspreet Kaur,[a] Shaokui Ge,[a] Adler R. Dillman,[b] Nicholas V. DiPatrizio,[a] Meera G. Nair[a]

[a]Division of Biomedical Sciences, University of California, Riverside, Riverside, California, USA
[b]Department of Nematology, University of California, Riverside, Riverside, California, USA
[c]Institute of Health Informatics, University of Minnesota, Minneapolis, Minnesota, USA

ABSTRACT Helminths have coevolved with their hosts, resulting in the development of specialized host immune mechanisms and parasite-specific regulatory products. Identification of new pathways that regulate helminth infection could provide a better understanding of host-helminth interaction and may identify new therapeutic targets for helminth infection. Here we identify the endocannabinoid system as a new mechanism that influences host immunity to helminths. Endocannabinoids are lipid-derived signaling molecules that control important physiologic processes, such as feeding behavior and metabolism. Following murine infection with *Nippostrongylus brasiliensis*, an intestinal nematode with a life cycle similar to that of hookworms, we observed increased levels of endocannabinoids (2-arachidonoylglycerol [2-AG] or anandamide [AEA]) and the endocannabinoid-like molecule oleoylethanolamine (OEA) in infected lung and intestine. To investigate endocannabinoid function in helminth infection, we employed pharmacological inhibitors of cannabinoid subtype receptors 1 and 2 (CB_1R and CB_2R). Compared to findings for vehicle-treated mice, inhibition of CB_1R but not CB_2R resulted in increased *N. brasiliensis* worm burden and egg output, associated with significantly decreased expression of the T helper type 2 cytokine interleukin 5 (IL-5) in intestinal tissue and splenocyte cultures. Strikingly, bioinformatic analysis of genomic and transcriptome sequencing (RNA-seq) data sets identified putative genes encoding endocannabinoid biosynthetic and degradative enzymes in many parasitic nematodes. To test the novel hypothesis that helminth parasites produce their own endocannabinoids, we measured endocannabinoid levels in *N. brasiliensis* by mass spectrometry and quantitative PCR and found that *N. brasiliensis* parasites produced endocannabinoids, especially at the infectious larval stage. To our knowledge, this is the first report of helminth- and host-derived endocannabinoids that promote host immune responses and reduce parasite burden.

KEYWORDS endocannabinoid, gastrointestinal helminth, nematode

Parasitic helminths infect an estimated two billion individuals worldwide (1). Although helminth infection is not typically fatal, it is associated with a multitude of pathological conditions, including malnutrition and growth retardation. A majority of soil-transmitted helminths reside in the gastrointestinal tract, where they can negatively impact the host's nutritional status by stealing nutrients or preventing nutrient absorption by damaging or causing inflammation of the intestinal tissue (2). Additionally, recent studies have identified new mechanisms by which helminths impact host feeding and metabolism (3). Gastrointestinal helminth infection was reported to decrease food intake (4) and was beneficial in mice fed a high-fat diet, in which it improved glucose metabolism and reduced adiposity (5, 6). This effect was partly mediated through T helper type 2 (Th2) cytokine-activated M2 macrophages in the

Received 6 June 2018 **Accepted** 7 August 2018

Accepted manuscript posted online 13 August 2018

Citation Batugedara HM, Argueta D, Jang JC, Lu D, Macchietto M, Kaur J, Ge S, Dillman AR, DiPatrizio NV, Nair MG. 2018. Host- and helminth-derived endocannabinoids that have effects on host immunity are generated during infection. Infect Immun 86:e00441-18. https://doi.org/10.1128/IAI.00441-18.

Editor John H. Adams, University of South Florida

Address correspondence to Nicholas V. DiPatrizio, ndipatri@medsch.ucr.edu, or Meera G. Nair, meera.nair@ucr.edu.

H.M.B., D.A., and J.C.J. contributed equally to this article. N.V.D. and M.G.N. also contributed equally to this article.

adipose tissue, which have a known beneficial effect on metabolic homeostasis (7). In the intestine, helminth infection induced a Th2 cytokine-dependent expansion of tuft cells, which express taste receptors, and cholecystokinin (CCK)-positive enteroendocrine cells, which secrete hormones that regulate feeding behavior (8). Overall, these findings support a multifactorial relationship between helminth and host immune response that affects host feeding behavior and metabolism. Identification of new helminth or host-derived factors that regulate this process, and how they affect host health and helminth killing, could provide a better understanding of the pathological or beneficial effects of helminth infection that could be exploited therapeutically.

Among the many host-derived molecules that affect feeding and metabolism, endocannabinoids are an important class of lipid molecules that regulate these physiological processes (9, 10). Endocannabinoids are the body's natural cannabis-like molecules that signal through cannabinoid receptors, which are highly expressed on neurons (11). Unsurprisingly, a highly recognized function of endocannabinoids is promoting neurally mediated behaviors such as food intake and reward (9). Endocannabinoids, however, are generated throughout the body, and cannabinoid receptors are present on extraneuronal cells, including intestinal epithelial cells and immune cells (12–14). Signaling by the endocannabinoids, 2-arachidonoylglycerol (2-AG) and anandamide (AEA), through cannabinoid receptors on intestinal cells impacts feeding behavior (15, 16), while signaling on immune cells can promote anti-inflammatory pathways (17). Despite functional effects on intestinal physiology and immune responses, no studies reported to date have investigated the role of endocannabinoids in parasite infection.

In this study, we investigated the expression and function of endocannabinoids in murine infection with *Nippostrongylus brasiliensis*, a rodent nematode parasite that has a life cycle similar to that of human hookworms (18). We show that *N. brasiliensis* infection significantly induces the biosynthesis of endocannabinoids and endocannabinoid-like molecules in the infected lung and intestine. We also performed functional assays to measure endocannabinoid biosynthetic and degradative enzyme activity in infected jejunal tissue, and we observed significantly increased endocannabinoid synthetic but not degradative enzyme activity. Endocannabinoid levels were negatively correlated with early infection-induced weight loss, associated with reduced food intake, and *N. brasiliensis* egg output, suggesting that endocannabinoids are associated with improved host immunity. To test this hypothesis, we employed validated peripheral pharmacological inhibitors of the cannabinoid subtype 1 receptor (CB_1R) and CB_2R, AM6545 and AM630, respectively, which act peripherally and do not cross the blood-brain barrier (16, 19). Pharmacological inhibition of CB_1R, but not CB_2R, significantly increased *N. brasiliensis* worm burdens and fecal egg output. Increased parasite burden was associated with reductions in Th2 cytokines (interleukin 5 [IL-5] and IL-4) but not in the Th1 cytokine gamma interferon (IFN-γ), suggesting that *N. brasiliensis*-induced endocannabinoid signaling through CB_1R was important for optimal host Th2 immune responses. Strikingly, bioinformatic analyses of the genomes and transcriptome sequencing (RNA-seq) data sets from *N. brasiliensis* and other parasitic nematodes, including the hookworms *Ancylostoma ceylanicum* and *Necator americanus*, revealed putative genes encoding endocannabinoid synthetic and degradative enzymes. We validated the bioinformatic predictions for *N. brasiliensis* by quantitative real-time PCR and mass spectrometry (MS) and showed that *N. brasiliensis* produces endocannabinoids at all life cycle stages. Taken together, these studies show for the first time the production of endocannabinoids by parasitic helminths and suggest that helminth infection-induced endocannabinoids functionally influence the host immune response and parasite burden. These findings support a new area of investigation into the function of the endocannabinoid system in infectious diseases.

RESULTS

***Nippostrongylus brasiliensis* infection induces lung and intestinal endocannabinoid production.** Endocannabinoids are lipid signaling mediators that affect a variety of behaviors (e.g., feeding and memory) and metabolic processes (e.g., glucose ho-

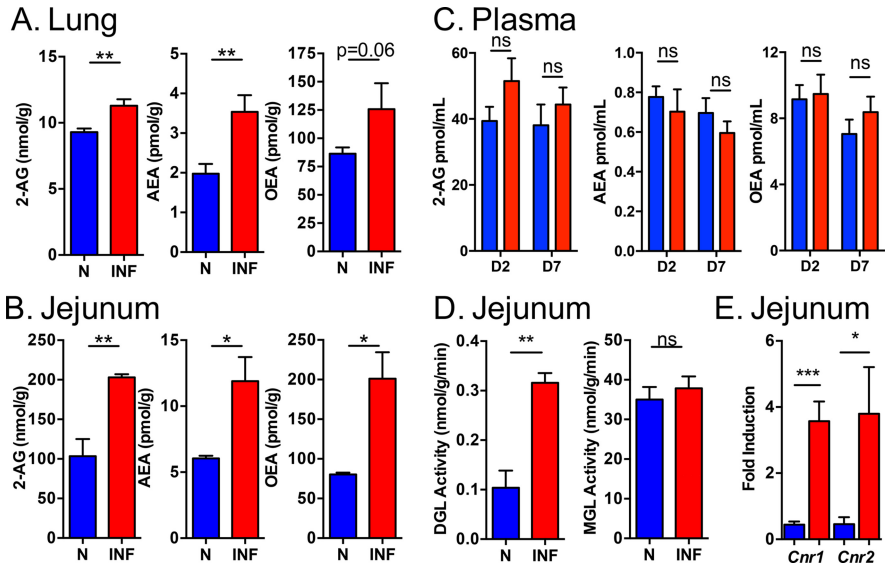

FIG 1 *N. brasiliensis* infection induces endocannabinoid production and cannabinoid receptor expression. C57BL/6 mice were left naive or infected for 2 or 7 days with 500 *N. brasiliensis* L3 worms. 2-AG, AEA, and OEA levels in the lung at day 2 (A), jejunum at day 7 (B), and plasma at day 2 and day 7 (C). (D) 2-AG biosynthetic (DGL, left) and degradative (MGL, right) enzyme activities were measured in jejunal tissue from naive or day 7 infected mice. (E) *N. brasiliensis* infection-induced *Cnr1* and *Cnr2* mRNA in the jejunal tissue at day 7 was quantified as fold induction over naive after normalization with the 18S rRNA housekeeping gene. Data are presented as means ± SEM (n = 4 to 6/group) and are representative of results from four experiments.

meostasis) (see Fig. S1 in the supplemental material) (9). Additionally, endocannabinoids can regulate the immune response and dampen inflammation (20). Despite reported immunoregulatory function, however, whether endocannabinoids are generated in parasite infection and the functional consequence for the host or pathogen are unknown. *N. brasiliensis* infects the small intestine of mice and has been shown to affect food intake and metabolism (3–5). Given that endocannabinoids and endocannabinoid receptors are expressed in the intestine, we hypothesized that *N. brasiliensis* infection may affect endocannabinoid signaling. Similar to the hookworm life cycle, *N. brasiliensis* infects both the lung and the intestine as part of its life cycle and feeds on host blood (21). We therefore measured tissue and circulating endocannabinoid levels in naive and *N. brasiliensis*-infected mice at days 2 and 7 postinfection, when the parasites had infected the lung and jejunum, respectively. We observed a modest but significant increase in 2-AG and AEA in *N. brasiliensis*-infected lung tissue and a trend toward increased levels of endocannabinoid-like molecule oleoylethanolamine (OEA) (Fig. 1A). Strikingly, 2-AG levels in jejunal tissue were almost 10-fold higher than in the lung, and we observed a >2-fold increase following *N. brasiliensis* infection (Fig. 1B). AEA and OEA, both of which regulate feeding and are anti-inflammatory (15, 22, 23), were also significantly elevated in the jejunum in response to *N. brasiliensis* infection (Fig. 1B). In contrast, circulating endocannabinoid levels in the plasma were unchanged following *N. brasiliensis* infection (Fig. 1C), suggesting that *N. brasiliensis*-induced endocannabinoids were restricted to the tissue infection site. Given that the 2-AG levels were highest in the infected jejunum, we next evaluated the activity of the biosynthetic and degradative enzymes responsible for 2-AG metabolism in jejunal epithelium of infected versus naive mice. Specifically, we measured the enzymatic activities of diacylglycerol lipase (DGL; biosynthetic) and monoacylglycerol lipase (MGL; degradative) by functional enzyme assays (15). We found significant increases in the activity of DGL in the jejunal tissue of infected mice compared to noninfected mice (Fig. 1D, left), which suggests that levels of 2-AG in jejunum are elevated in infected mice by a mechanism that includes increases in jejunal DGL-mediated 2-AG biosynthesis. In contrast, we did not observe any changes in enzymatic activity of MGL (Fig. 1D, right). Endocannabi-

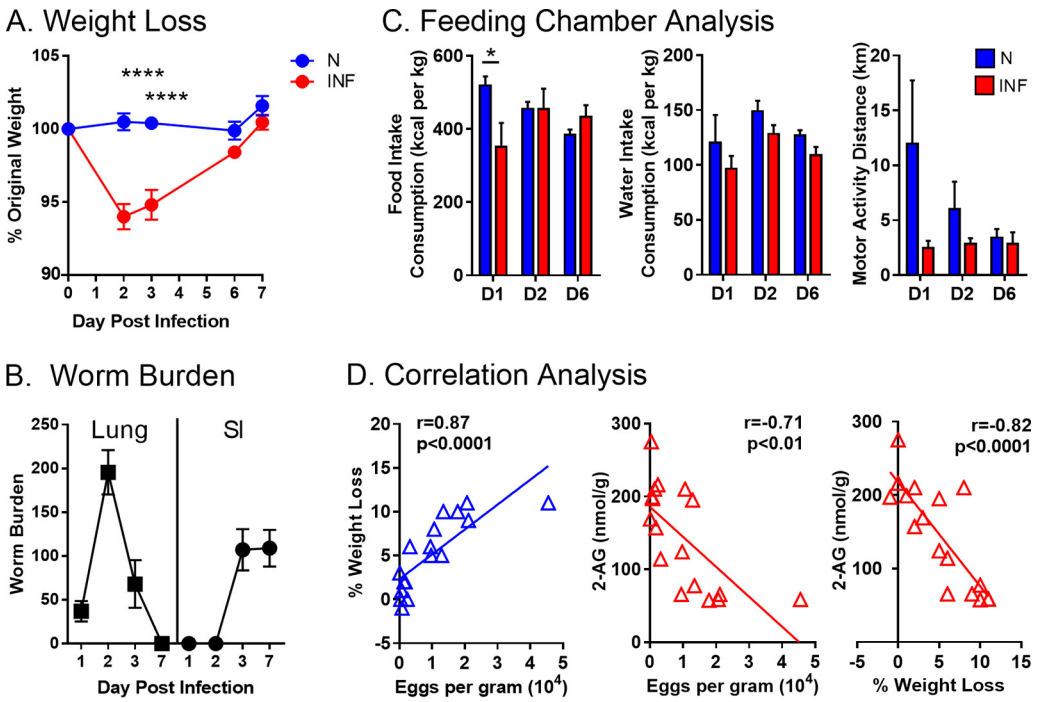

FIG 2 Intestinal endocannabinoid levels are negatively correlated with infection-induced weight loss and fecal egg burdens. (A) Time course of *N. brasiliensis* infection-induced weight loss. (B) Compiled data of *N. brasiliensis* parasite burdens in lung and small intestine. (C) Food, water intake, and motor activities of naive (N) and *N. brasiliensis*-infected (INF) mice were evaluated in a feeding chamber. (D) Correlation analysis between parasite egg burden and weight loss (left) and jejunal 2-AG (right) was performed. Data are presented as means ± SEM and are representative of results from two to four experiments ($n = 4$ to 6/group).

noids signal through the G protein-coupled cannabinoid receptors subtype 1 and 2; therefore, we measured the cannabinoid receptor coding genes *Cnr1* and *Cnr2* mRNA by quantitative PCR of the jejunal tissue. *N. brasiliensis* infection induced significant increases in both *Cnr1* and *Cnr2* (Fig. 1E). Collectively, these data demonstrate that *N. brasiliensis* infection increases endocannabinoid levels locally in the infected lung and intestinal tissue and promotes intestinal endocannabinoid receptor expression, suggesting that the endocannabinoid system is induced in helminth infection.

Intestinal endocannabinoids are negatively correlated with *Nippostrongylus brasiliensis* infection-induced weight loss and parasite egg burdens. We examined if *N. brasiliensis*-induced endocannabinoids were associated with health outcomes for the host or parasite by correlative analyses between endocannabinoid levels and infection-induced weight loss or parasite egg burdens. *N. brasiliensis* infectious larval stage 3 (L3) helminths migrate to the lung, where they develop into L4, followed by infection of the small intestine, where they develop into adults and produce eggs (Fig. 2A and B). At an infectious dose of 500 L3 helminths, *N. brasiliensis* infection of the lung, which occurs between days 1 and 3 postinfection, causes lung hemorrhaging and inflammation likely due to the physical damage of the worm burrowing through the lung tissue. During this acute infection of the lung, we observed significant weight loss that was remarkably resolved once the *N. brasiliensis* parasites were established in the intestine, at day 6 (Fig. 2A). Consistent with this weight loss, analysis of feeding patterns in naive and infected mice revealed reduced food intake ($P < 0.05$) and motor activity ($P = 0.05$) at day 1 postinfection, when the *N. brasiliensis* parasites had reached the lung, that was also resolved by day 6 postinfection (Fig. 2C). We also observed a significant positive correlation between *N. brasiliensis*-induced acute weight loss at day 3 and *N. brasiliensis* egg burdens at day 7 postinfection (Fig. 2D, left). This correlation suggests that acute infection-induced weight loss at day 3 may be a good predictor of subsequent parasite establishment in the intestine. The effect of *N. brasiliensis* infection

TABLE 1 Correlation analysis between endocannabinoids from day 7 *N. brasiliensis*-infected mice, day 3 infection-induced weight loss, and day 7 parasite egg burden[a]

Parameter	Value or statistical significance for:					
	Jejunum eCB			Plasma eCB		
Weight loss	2-AG	AEA	OEA	2-AG	AEA	OEA
Spearman *r*	−0.8154	−0.3678	−0.7159	0.7688	0.3617	0.7269
P value	***	NS	**	***	NS	**
Egg burden						
Spearman *r*	−0.7137	−0.4265	−0.6593	0.7279	0.1878	0.6127
P value	**	NS	**	**	NS	*

[a]$n = 17$. eCB, endocannabinoids; NS, not significant.

on mouse weight changes may be due to lung tissue inflammation or changes in mouse feeding behavior.

Given that endocannabinoids can regulate both these processes, we investigated correlations between endocannabinoids and *N. brasiliensis* parasite burdens. We observed that 2-AG intestinal levels from day 7 infected mice were negatively correlated with early infection-induced weight loss (day 3) and day 7 parasite egg burden (Fig. 2D, right). To comprehensively define the relationship between endocannabinoids versus host and parasite fitness, we performed Spearman correlation analyses across all experiments (Table 1). We observed a negative correlation between day 7 infected jejunum 2-AG and OEA and (i) early (day 3) infection-induced weight changes and (ii) day 7 parasite egg burden. In contrast, we observed a positive correlation between plasma 2-AG and OEA, weight loss, and parasite egg burden. These data indicate that high endocannabinoid levels locally in the intestine are associated with reduced early infection-induced weight loss and decreased parasite egg burden.

Disruption of CB_1 receptor but not CB_2 receptor signaling increases *Nippostrongylus brasiliensis* egg burden and impairs intestinal IL-5 responses. The endocannabinoids, 2-AG and AEA, both of which were upregulated following *N. brasiliensis* infection (Fig. 1), signal through CB_1R and CB_2R (12). We investigated the function of endocannabinoid signaling in *N. brasiliensis* infection by treatment with the peripherally restricted neutral CB_1R antagonist AM6545 (24, 25), CB_2R antagonist AM630 (19), and dimethyl sulfoxide (DMSO) as a vehicle control. To rule out potential confounding effects on parasite establishment in the intestine, mice were treated daily with antagonists or vehicle starting at day 4 postinfection, when all *N. brasiliensis* parasites had reached the intestine. At this time point, CB_1R or CB_2R inhibition had no effect on mouse weight (Fig. 3A). Interestingly, CB_1R but not CB_2R inhibition led to increased fecal *N. brasiliensis* egg output and intestinal *N. brasiliensis* worm counts (Fig. 3B), suggesting that CB_1R signaling is necessary for optimal *N. brasiliensis* explusion. We validated these CB_1R inhibitor-mediated differences in *N. brasiliensis* burdens across three experimental repeats, using generalized linear models, and found that CB_1R inhibitor treatment led to a 2.21-fold-higher egg burden ($P = 0.01$) and 1.46-fold-higher worm burden ($P < 0.01$) (Table 2). CB_1R inhibition resulted in significantly decreased intestinal levels of the Th2 cytokine IL-5 but not IL-4, IFN-γ, or IL-10 (Fig. 3C). Further, *in vitro* CD3/CD28-activated splenocytes from CB_1R inhibitor-treated mice secreted significantly less IL-5, IL-4, and IL-10 than vehicle-treated mice but exhibited no defect in IFN-γ secretion (Fig. 3D). This cytokine effect was specific to CB_1R signaling, as inhibition of CB_2R signaling had no significant effect. Given that host immunity to *N. brasiliensis* is dependent on Th2 cytokines, the CB_1R inhibitor-induced decrease in IL-5 and IL-4 may explain the increase in parasite egg burden. Additionally, the significant reduction in IL-10 secretion is consistent with an anti-inflammatory function for CBR signaling (22). These data support the functional link between the endocannabinoid system and immunity to *N. brasiliensis* and suggest that CB_1R signaling has a beneficial impact for the host following *N. brasiliensis* infection by promoting Th2 cytokine expression and reducing parasite burdens.

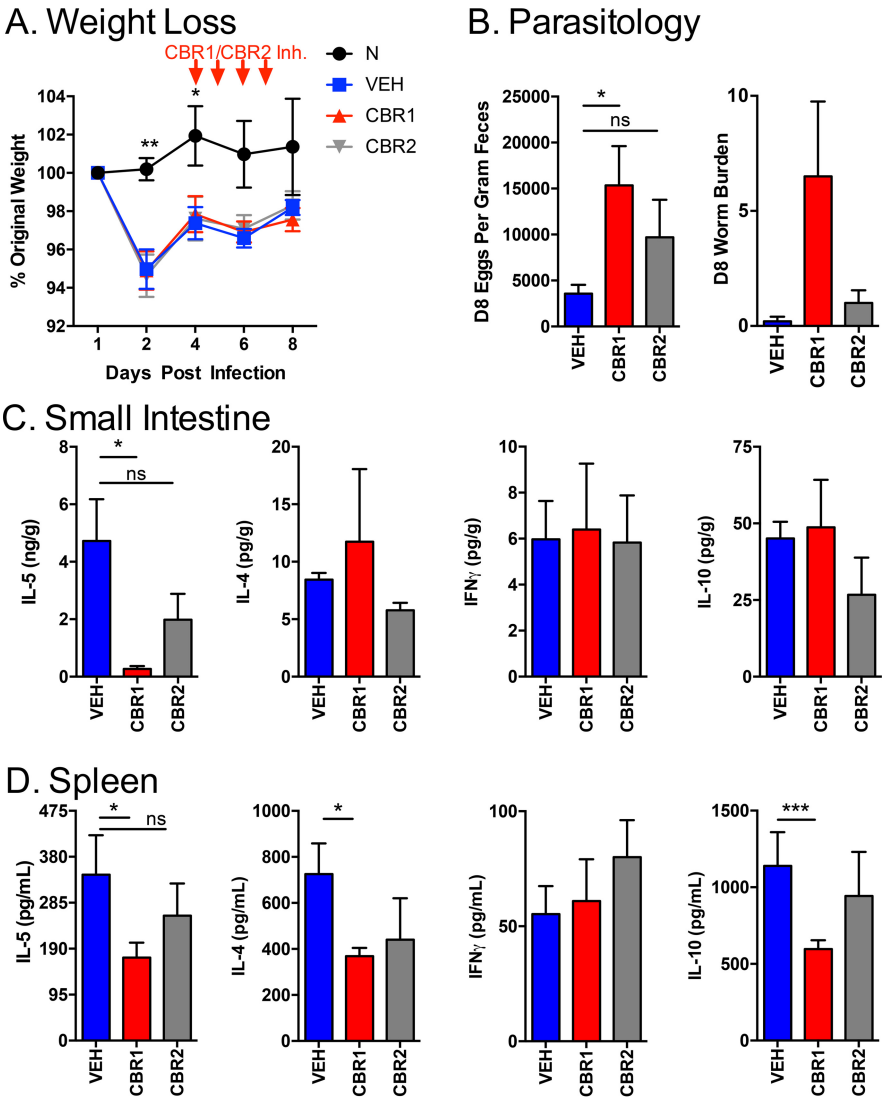

FIG 3 Pharmacological inhibition of cannabinoid receptor 1 but not cannabinoid receptor 2 increases helminth burdens associated with decreased IL-5 expression. C57BL/6 mice were left naive (black) or infected with *N. brasiliensis*. At days 4 to 7 postinfection, mice were treated intraperitoneally with AM6545 (CB1 inhibotor [Inh]; red), AM630 (CB2 inhibitor; gray), or DMSO (VEH; blue). (A) Infection-induced weight loss was monitored and compared to that in naive mice. (B) Fecal egg burdens (left) and intestinal worm counts (right) were quantified in *N. brasiliensis*-infected mice. (C and D) IL-5, IL-4, IFN-γ, and IL-10 were quantified in day 8 infected (C) intestinal tissue homogenate and (D) supernatant from 72-h anti-CD3/anti-CD28-stimulated splenocytes. Data are presented as means ± SEM (n = 4 to 6/group) and representative of results from three separate experiments.

The endocannabinoid system is present in *Nippostrongylus brasiliensis* and other parasitic helminths. The endocannabinoid system is conserved in vertebrates and some invertebrates (26), and endocannabinoid biosynthetic and degradative enzymes are expressed in *Caenorhabditis elegans* (27). However, whether the endocannabinoid system exists in parasitic helminths is unknown. We conducted bioinformatic

TABLE 2 Effect of CBR1 inhibitor on *N. brasiliensis* egg and worm burden estimated by linear regression models[a]

CB1 inhibitor effect	Effect estimation	95% confidence interval	*P* value
Egg burden	2.21	1.25 to ~3.91	0.01
Worm count	1.46	1.29 to ~1.64	<0.001

[a]n = 16 to 18/group.

TABLE 3 Putative genes in endocannabinoid signaling and degradation identified in the genomes of *N. brasiliensis*, human hookworms, and other parasitic nematodes

Gene	Present in:								
	N. brasiliensis	*A. duodenale*	*A. ceylanicum*	*N. americanum*	*S. carpocapsae*	*A. lumbricoides*	*S. ratti*	*S. stercoralis*	*T. canis*
npr-19	X	√	√	√	√	√	√	√	√
nape-1	√	√	√	√	√	√	X	X	√
faah-1	√	√	√	√	√	√	√	√	√
dagl-2	√	√	√	√	√	√	√	√	√
magl	X	X	X	X	X	X	X	X	X
abhd-6	√	√	√	√	√	√	√	√	√
abhd-12	√	√	√	√	√	√	√	√	√
abhd-5	√	√	√	√	√	√	√	√	√

analyses of available parasitic nematode genomes for genes involved in the endocannabinoid synthetic and signaling pathway (Table 3). Within the *N. brasiliensis* genome, genes encoding synthetic enzymes for the monoacylglycerols, 2-AG and DHAG (*dagl*), and the fatty acid ethanolamides, AEA, OEA, and docosahexaenoylethanolamide (DHEA) (*nape*), were identified. We also found orthologs of the fatty acid ethanolamide degradative enzyme fatty acid amide hydrolase (*faah-1*), the proposed monoacylglycerol degradative enzymes alpha beta hydroxylases (*abhd-12* and *abhd-5*). Although nematodes did not have obvious orthologs of monoacylglycerol lipase (*magl*), the major degradative enzyme for 2-AG found in mammals, we identified a putative nematode gene encoding the minor 2-AG degradative enzyme, *abhd-6* (28). Moreover, the synthetic and degradative endocannabinoid genes were conserved in other nematodes, including the human hookworms *Ancylostoma duodenale* and *Necator americanus* and human roundworm *Ascaris lumbricoides*.

Analysis of available RNA-seq data sets revealed the expression of putative genes for the endocannabinoid pathway in parasitic nematodes of humans (*A. ceylanicum*, *Ascaris suum*, *N. americanus*, *Toxocara canis*, and *Strongyloides stercoralis*), rodents (*N. brasiliensis* and *Strongyloides ratti*), and even insects (*Steinernema carpocapsae*) (Fig. 4; see also Fig. S2 in the supplemental material). Further, these genes were expressed in a tissue- or stage-specific manner in some of these parasites. For example, the hookworm *A. ceylanicum*, which infects humans and other mammals, showed expression of *abhd-5* in all stages sampled but showed highest expression of *abhd-5* in the infective L3 stage. In the human hookworm *N. americanus*, both *nape-1* and *abhd-12* were more highly expressed in L3 larvae than in adult nematodes. Although it was previously thought that no obvious orthologs of CB_1 and CB_2 receptors were present in nematodes, a recent study identified the neuropeptide receptor NPR-19 as a cannabinoid-like receptor in *C. elegans* (29–33). We were able to find putative orthologs of the cannabinoid-like receptor NPR-19 in other nematodes, including *A. ceylanicum*, *N. americanus*, and *Wuchereria bancrofti* (Table 3). However, we were not able to find an obvious ortholog of NPR-19 in *N. brasiliensis*, though this may be due to the incomplete state of the available *N. brasiliensis* genome (N50 = 33.5 kb; i.e., nearly 30% of the predicted protein-coding genes are on contigs smaller than 10 kb), rather than the absence of an NPR-19 ortholog (34, 35).

***Nippostrongylus brasiliensis* produces endocannabinoids.** Given the presence of genes encoding endocannabinoid synthetic and degradative enzymes in the *N. brasiliensis* genome, we investigated if *N. brasiliensis* could produce endocannabinoids at any stage of its life cycle. We isolated infectious *N. brasiliensis* L3 worms from hatched fecal cultures, *N. brasiliensis* L4 worms from day 2 infected lungs, and *N. brasiliensis* adults from day 7 infected jejunum, performed thorough washes in phosphate-buffered saline (PBS), and measured endocannabinoid levels. Although there were no endocannabinoids in the control washes, we measured detectable levels of endocannabinoids and endocannabinoid-like molecules in worm extracts from all life cycle stages (Fig. 5A). These exhibited identical chromatogram patterns to reference endocannabinoids, AEA (Fig. 5B) and 2-AG (Fig. 5C), and endocannabinoid-like molecules (see Fig. S3A to C in

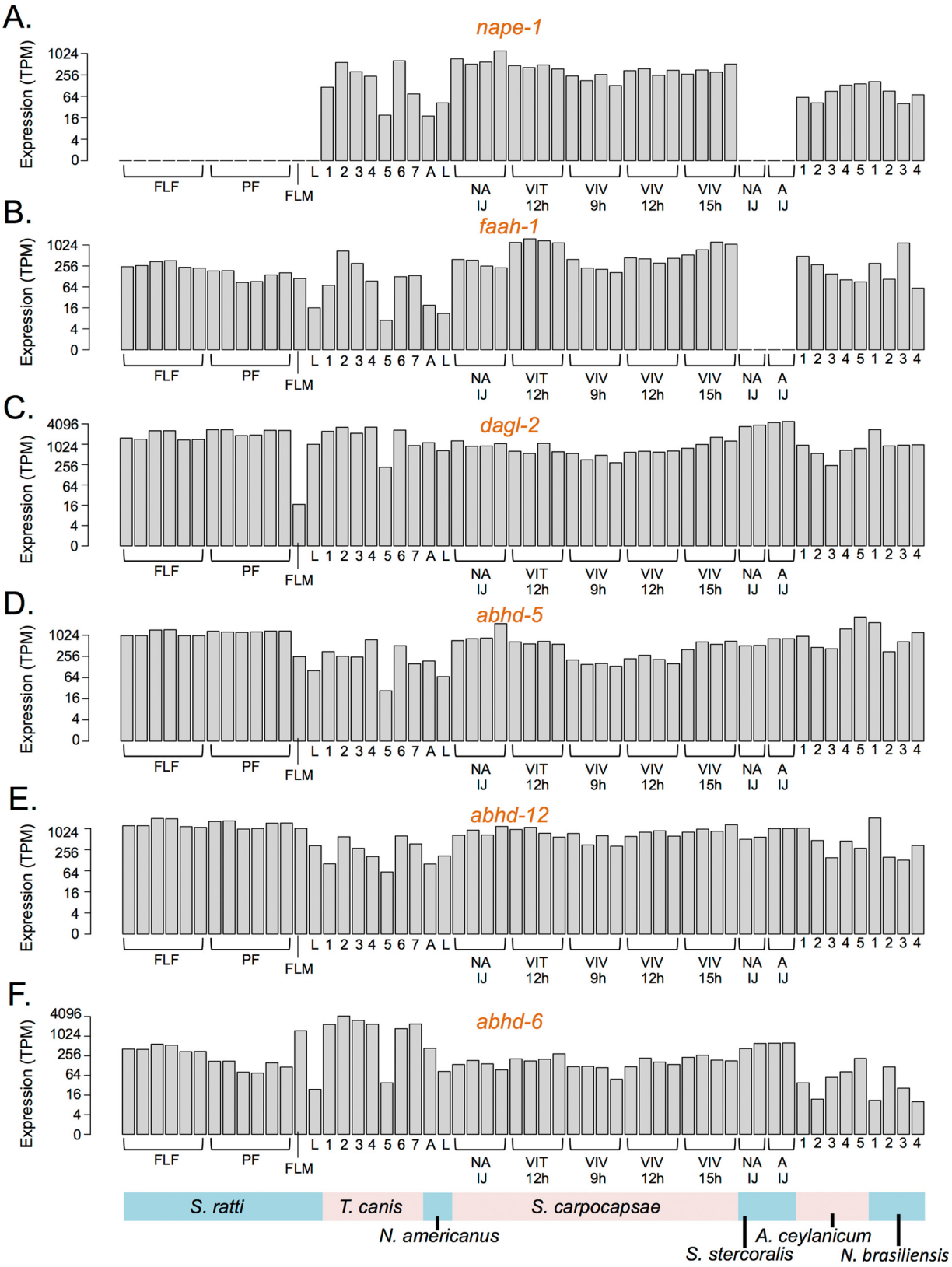

FIG 4 Expression of genes encoding endocannabinoid biosynthetic and degradative enzymes in parasitic nematodes. Nematode expression data for endocannabinoid biosynthetic enzyme gene *nape-1* (A) and degradative enzyme gene *faah-1* (B), the monoacylglycerol biosynthetic enzyme gene *dagl-2* (C), and genes for the potential degradative enzymes alpha beta hydrolases (*abhd-5* [D] and *abhd-12* [E]) and the minor 2-AG degradative enzyme (*abhd-6* [F]) are shown in transcripts per million (TPM). The life stages for *S. ratti* expression are: free-living female (FLF), parasitic female (PF), free-living male (FLM), and infective L3 (L). The tissues for expression data for *T. canis* expression are female gut (1), female

(Continued on next page)

the supplemental material). On a per-weight basis, adult *N. brasiliensis* produced the most 2-AG and DHAG, whereas L4 worms produced OEA. Strikingly, infectious L3 worms produced over 100-fold more AEA than the other life cycle stages or the host (Fig. 1B). L4 and adult *N. brasiliensis* worms feed on host tissue and blood; therefore, it may be possible that some endocannabinoids detected may be host derived. However, the infectious L3 worms were isolated from culture and concentrations of AEA reached 1,000 pmol per gram of worm, which is 100 to 200 times the level found in upper intestinal mucosal scrapings (5 to 10 pmol per g of tissue) and 300 to 1,000 times found in circulation (1 to 3 pmol per ml) (Fig. 1 and reference 16). Thus, the endocannabinoids measured in L3 worms were likely generated by the parasite. Consistent with the presence of a functional endocannabinoid system in *N. brasiliensis*, sequence alignment of the predicted *N. brasiliensis* gene encoding NAPE-PLD, the dominant enzyme catalyzing the biosynthesis of fatty acids ethanolamides, including AEA, OEA, and DHEA, revealed 43% identity and sequence conservation in the functional lactamase domain (Fig. 5D). To validate that the predicted *N. brasiliensis* genes encoding endocannabinoid biosynthetic and degradative enzymes were expressed, we performed quantitative PCR for predicted *nape* and *faah* and the actin gene as a housekeeping gene control (Fig. 5E). *nape* and *faah* mRNAs were present in all *N. brasiliensis* life cycle stages, with the highest expression in the infectious L3 stage. Overall, these data show for the first time that endocannabinoids are produced by *N. brasiliensis* and suggest that the endocannabinoid system is also present in parasitic nematodes that infect humans.

DISCUSSION

In this study, we investigated the endocannabinoid signaling system following infection with *N. brasiliensis*. While recognized for its critical function in the central and enteric nervous systems, the endocannabinoid system is also activated by and can influence inflammatory immune responses (20, 36, 37). For example, 2-AG and AEA are anti-inflammatory, which has provided the basis for the potential therapeutic use of synthetic cannabinoids, or cannabis, in autoimmune or inflammatory diseases (38). Oral treatment of mice with AEA promoted a tolerogenic immune response and regulatory macrophages in the intestine that were protective in a nonobese diabetic model (39). Despite an immune function in the intestine, the functional significance of endocannabinoids in intestinal parasite infection has not been examined. Our finding that helminth infection triggers significant endocannabinoid synthesis that is correlated with both host health outcomes and parasite fecundity suggests that endocannabinoids may be an important player in host-helminth dynamics.

Inhibition of CB_1R led to decreased expression of the Th2 cytokine IL-5 in the intestine and IL-4, IL-5, and IL-10 in the spleen but no difference in the Th1 cytokine IFN-γ. This was associated with increased parasite egg and worm burdens, suggesting that CB_1R signaling may be important for the optimal host immune response to keep helminth burdens in check. Endocannabinoids also signal through CB_2R (20); however, CB_2R antagonist treatment did not significantly change cytokine responses or helminth burdens. CB_1R and CB_2R inhibition was conducted during a short time frame, days 4 to 6 postinfection, and we cannot confirm complete abrogation of CB_1R or CB_2R signaling in the intestine with this treatment regime. Future studies with earlier treatment regimes or CB_1R/CB_2R-deficient mice may delineate functional differences between these signaling pathways in helminth infection. Cannabinoid CB_1Rs are expressed in cholecystokinin (CCK)-positive enteroendocrine cells in the duodenum of mice (40) and ghrelin-expressing cells of the stomach of rats (41), and *N. brasiliensis* infection in rats

FIG 4 Legend (Continued)
reproductive tract (2), female anterior body (3), male gut (4), male reproductive tract (5), male anterior body (6), and L3 (7). The life stages for *N. americanus* expression are adult (A) and infectious L3 (L). The life stages for *S. carpocapsae* expression are nonactivated infective juveniles (IJs) (NA IJ), 12-h *in vitro* activated IJs (VIT 12 h), 9-h *in vivo* activated IJs (VIV 9h), 12-h *in vivo* activated IJs (VIV 12h), and 15 h *in vivo* activated IJs (VIV 15h). The life stages for *S. stercoralis* expression are nonactivated IJ (NA IJ) and activated IJ (A IJ). The life stages for *A. ceylanicum* expression are 17 days postinfection (1), 12 days postinfection (2), 5 days postinfection (3), 24-h incubation in hookworm culture media (4), and infective L3 (5). The life stages for *N. brasiliensis* expression are adult (1), L4 from mouse lung (2), infectious L3 (3), and eggs (4).

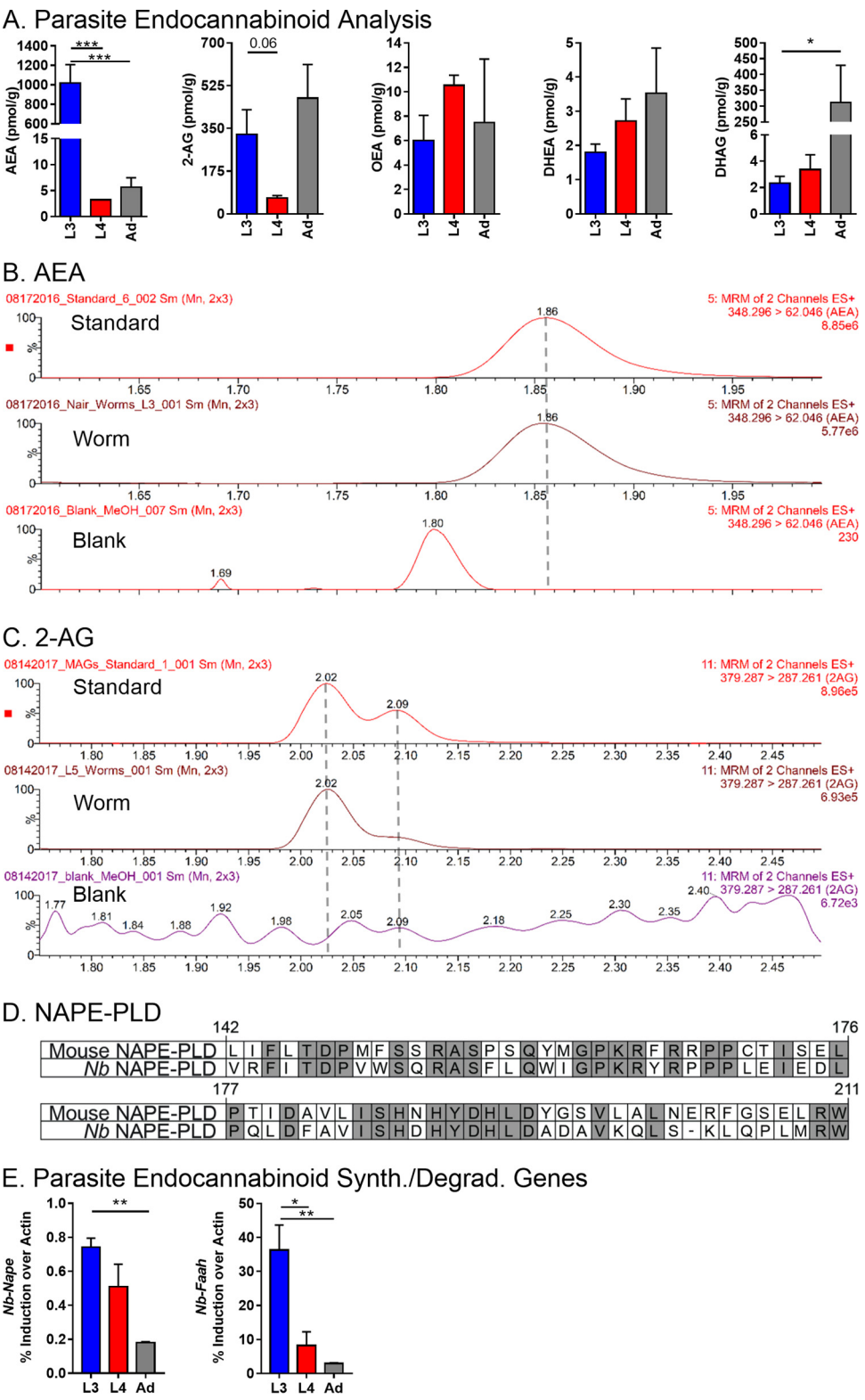

FIG 5 *N. brasiliensis* produces endocannabinoids and cannabinoid-like molecules. *N. brasiliensis* parasites from life cycle stages were isolated, washed, and assessed for levels of endocannabinoids and endocannabinoid-like molecules by UPLC/MS/MS. (A) Levels of analytes at various life stages: anandamide (AEA), 2-arachidonoyl-*sn*-glycerol (2-AG), oleoylethanolamide (OEA), docosahexaenoylethanolamide (DHEA), and docosahexaenoylglycerol (DHAG). (B and C) Representative chromatograms of AEA (B) and 2-AG (C). (D) A 68-amino-acid (aa) region of an alignment of mouse and *N. brasiliensis* NAPE-PLD (43% shared identity). The alignment region shown is the first 68 aa in a 202-aa lactamase (B_2) domain identified in mouse NAPE-PLD. (E) Quantitative reverse transcription-PCR of *Nippostrongylus* life cycle stages for predicted *nape* and *faah*.

is associated with elevations in circulating levels of CCK (4, 42). Thus, it is possible that helminth infection may induce changes in feeding behavior, as seen in Fig. 2, by a mechanism that includes endocannabinoid-mediated changes in the production and/or release of peptides important for feeding behavior, including CCK. We observed significant correlations between endocannabinoid levels, infection-induced weight loss, and parasite burdens. However, further functional studies are necessary to determine causal relationships between these multiple parameters and the contribution, if any, of infection-induced endocannabinoids to feeding behavior.

In addition to host endocannabinoid expression, we show for the first time that *N. brasiliensis* produces endocannabinoids and that genes encoding endocannabinoid biosynthetic and degradative enzymes are present in the genomes of multiple parasitic nematodes, including some of the most common helminth parasites of humans. One proposed strategy by which parasites modulate host immunity is by releasing molecules that are already native within the host, or at least native-like molecules (43). For example, *A. suum* and *T. canis* have been shown to synthesize morphine or morphine-like substrates, and morphine is a known immunomodulator (44, 45). It is well recognized that the endocannabinoid system is conserved in a diverse variety of vertebrates, including pythons (46) and goldfish (47); however, whether it evolved earlier and is functional in more primitive eukaryotic organisms is less well understood (29). We observed that *N. brasiliensis* has predicted genes encoding the NAPE-PLD and FAAH enzymes that catalyze endocannabinoid synthesis and breakdown. Quantitative PCR analysis confirmed *N. brasiliensis* expression of both of these predicted genes. Moreover, mass spectrometry analysis revealed that infectious L3 *N. brasiliensis* produced extremely high levels of AEA, reaching 100 to 1,000 times that found in tissue or blood of mice. A recent study showed that truffles, the fruiting bodies of fungi, produce AEA potentially as an attractant and feeding stimulant for animals to ensure its dissemination (48). Given that AEA is anti-inflammatory, high-level synthesis at the infectious stage may also function to dampen the host immune response. It is possible that in addition to endocannabinoids, *N. brasiliensis* may produce and release other signaling molecules endogenous to the host, such as morphine, and that there is overlap in the biological effects of these molecules on host immunity or behavior. Given the difference in mass between *N. brasiliensis* and the host, the endocannabinoids detected in the infected mice are likely host derived. However, it is possible that *N. brasiliensis*-derived endocannabinoids may functionally impact the host at the cellular level. Future studies are necessary to test these hypotheses.

Inhibition of CB_1R signaling significantly increased *N. brasiliensis* egg burden; however, whether the functional effect was through influencing the host or alteration of the endocannabinoid system in *N. brasiliensis* is unclear. In the host, the increased *N. brasiliensis* burdens when CB_1R signaling is inhibited could be due to the altered immune response or to reduced intestinal motility. Indeed, immune cells express both CB_1 and CB_2 receptors (49) (i.e., macrophages, dendritic cells, and T cells) and intestinal epithelial cells express CB_1R (14). Whether the CB_1R inhibitor-mediated increase in *N. brasiliensis* burden was through direct effects on immune cells, effects on the intestinal epithelial cells, or a combination of such effects is unclear and would require further studies. In addition to regulating immune responses, the endocannabinoid system throughout the gastrointestinal tract plays a variety of physiological roles, including the control of motility, immune function, mucosal barrier function, and feeding behavior (50–52). Although outside the scope of the present study, future studies should include an evaluation of the impact that endocannabinoid-induced changes in intestinal motility have on egg burden. Furthermore, it is possible that endocannabinoid metabolism and/or release may be secondarily affected by perturbations in physiological responses governed by endocannabinoids themselves. It is also possible that CB_1R inhibition could directly affect *N. brasiliensis*. Although the *N. brasiliensis* genome does not have canonical cannabinoid receptor genes, genes encoding endocannabinoid degradative enzymes are present in the *N. brasiliensis* genome, suggesting that *N. brasiliensis* may also respond to the endocannabinoids it produces through an as-yet-

unidentified receptor. Consistent with this, *C. elegans* produces and responds to cannabinoids through NPR-19 (31–33). Inhibiting CB_1R signaling was ultimately beneficial to *N. brasiliensis*, leading to improved parasite fertility. Why *N. brasiliensis* would produce endocannabinoids that adversely affect its fertility is unclear at present. Our data, however, support a functional impact of the host and parasite endocannabinoid system and suggest that further studies delineating the beneficial or detrimental function of endocannabinoids in the host versus the helminth are warranted. For example, the timing of cannabinoid receptor signaling inhibition may be critical. In our studies, we inhibited CB_1R signaling after adult parasite establishment in the intestine; however, *N. brasiliensis* produces the most AEA during the initial infection, possibly as an anti-inflammatory mechanism to downregulate the host immune response. *N. brasiliensis*-derived AEA may also prevent excessive host inflammation that could lead to host mortality, which would be an equally adverse outcome for the helminth. Notwithstanding this, our discovery of parasite-derived endocannabinoids implicates the endocannabinoid system as a primitive pathway that contributes to host-pathogen interaction and suggests that investigation of the existence of the endocannabinoid system in other pathogens is warranted.

The complexity of host-helminth interaction and the numerous factors that influence the health outcomes for the parasite and the host are increasingly recognized. In addition to an optimized Th2 response for parasite expulsion, parasitic helminths trigger a multitude of nonimmune pathways that affect physiological processes, such as feeding and metabolism, but can also influence the immune response (53–55). Our findings suggest that the endocannabinoid system is a previously unrecognized contributor to this dynamic process and may therefore have a significant impact on the host's health outcome beyond parasite expulsion.

MATERIALS AND METHODS

Parasite. The *Nippostrongylus brasiliensis* life cycle was maintained in Sprague-Dawley rats, as previously described (56, 57). Hatched infectious L3 larvae were recovered from 1- to 2-week-old fecal egg cultures by a Baermann apparatus. L4 larvae were recovered from lung tissue of day 2 infected rats by manual picking from coarsely minced lung tissue in media after 2 h of incubation at 37°C. Adult *N. brasiliensis* parasites were recovered from day 6 to 8 *N. brasiliensis* infected rats by dissection and slitting of the whole small intestine, followed by 2 h of incubation in warm PBS and manual picking of the worms from the intestinal tissue or supernatant. Eggs in the feces of infected mice and rats were counted using a McMaster counting chamber. For endocannabinoid quantification, parasites were washed three times in excess PBS, counted, and weighed.

Mice and tissue recovery. C57BL/6 mice were purchased from the Jackson Laboratory or bred in-house. All mice in the experiment were age-matched (6- to 8-week-old) males and females housed in a specific-pathogen-free facility. Mice were anesthetized with isoflurane and injected subcutaneously with 500 *N. brasiliensis* L3 larvae. Behavior was assessed using single-housing units (TSE Systems, Chesterfield, MO). Mice were placed into units 3 days prior to recording for acclimation, and daily feeding was monitored using Phenomaster software (TSE Systems). Where indicated, mice were treated intraperitoneally with a vehicle control (7.5% DMSO, 7.5% Tween 80, and 85% saline), CB_1R antagonist AM6545 (10 mg/kg of body weight), or CB_2R antagonist AM630 (10 mg/kg). Blood recovery was done by cardiac puncture into tubes containing 7.2 mg of EDTA. Following excision of the small intestine, mucosa was stripped and recovered for endocannabinoid quantification. One-centimeter jejunal tissues were weighed and homogenized in 0.5 ml of PBS with Mini-Beadbeater-96 (BioSpec Products) at 4°C, and supernatants were collected after centrifugation (4,000 $\times$ *g* for 15 min at 4°C) for cytokine quantification. All protocols for animal use and euthanasia were approved by the University of California, Riverside Institutional Animal Care and Use Committee (https://or.ucr.edu/ori/committees/iacuc.aspx; protocols A-20150028E and A-20170036) and were in accordance with the National Institutes of Health guidelines. Animal studies are in accordance with the provisions established by the Animal Welfare Act and the *Public Health Service Policy on Humane Care and Use of Laboratory Animals* (71).

Lipid extraction and FAE and MAG analysis. Lipid extraction and analysis were performed as previously described (16, 36). Briefly, frozen tissue or worms (2,000 L3 worms/sample, 400 L4 worms/sample, and 100 adults/sample) were homogenized in 1.0 ml of methanol solution containing the internal standards $[^2H_5]$2-AG, $[^2H_4]$AEA, and $[^2H_4]$OEA (Cayman Chemical, Ann Arbor, MI). Lipids were extracted with chloroform (2 ml) and washed with water (1 ml). Lipids were similarly extracted from plasma samples, with the exception of a 0.9% saline wash replacing water (0.1 ml of plasma at the expense of saline). Organic phases were collected and separated by open-bed silica gel column chromatography as previously described (15). Eluate was gently dried under N_2 stream (99.998% pure) and resuspended in 0.1 ml of methanol-chloroform (9:1), with 1-μl injection for ultraperformance liquid chromatography-tandem mass spectrometry (UPLC/MS/MS) analysis.

Data were acquired using an Acquity I class UPLC with in-line connection to a Xevo TQ-S micro-triple-quadrupole mass spectrometer (Waters Corporation, Milford, MA) with electrospray ionization (ESI) sample delivery. Lipids were quantified using a stable isotope dilution method detecting proton or sodium adducts of the molecular ions $[M + H/Na]^+$ in multiple-reaction monitoring (MRM) mode. Extracted ion chromatograms for MRM transitions were used to quantify analytes 2-AG ($m/z = 379.3 > 287.3$), 2-docosahexaenoyl glycerol (2-DG) ($m/z = 403.3 > 311.2$), AEA ($m/z = 348.3 > 62.0$), OEA ($m/z = 326.4 > 62.1$), DHEA, ($m/z = 372.3 > 62.0$), 19:2 MAG ($m/z = 386.4 > 277.2$), with $[^2H_5]$2-AG ($m/z = 384.3 > 93.4$), $[^2H_4]$AEA ($m/z = 352.4 > 66.1$), and $[^2H_4]$OEA ($m/z = 330.4 > 66.0$) as internal standards. Controls included one "blank" sample that was processed and analyzed in the same manner as all samples, except that no tissue was included. This control revealed no detectable endocannabinoids and related lipids included in our analysis.

Functional enzyme assays of DGL and MGL activities. Data for free fatty acids (FFA) (19:2 FFA, product of the MGL assay) were measured using the UPLC/MS/MS instrument as described above. Mobile-phase compositions for 19:2 FFA were the same as described above, but the flow gradient began at a flow rate of 0.4 ml/min: 90% methanol for 0.1 min, 90% to 100% methanol for 0.1 to 2.0 min, 100% methanol for 2.0 to 2.1 min, 100% to 90% methanol for 2.1 to 2.2 min, and 90% methanol for 2.2 to 2.5 min. The product of DGL assay, 19:2 MAG, was analyzed exactly as described above for other MAGs. MS detection of fatty acids was in negative-ion mode with capillary voltage maintained at 1.10 kV. Cone voltages for respective analytes were as follows: 19:2 FFA, 48 V, and 17:1 FFA, 64 V. Lipids were quantified using a dilution series detecting deprotonated molecular ions in selected ion recording (SIR) mode. Extracted ion chromatograms for SIR masses were used to quantify the analyte 19:2 FFA ($m/z = 293.3$) and the internal standard 17:1 FFA ($m/z = 267.2$).

Tissue preparation. Intestinal epithelium was collected as described above, and approximately 100 mg of frozen tissue was homogenized in 2 ml of ice-cold 50 mM Tris-HCl–320 mM sucrose (pH 7.5) buffer. Homogenates were centrifuged at 800 $\times$ *g* for 10 min while kept at 4°C, and supernatant was collected. Protein supernatants were sonicated twice for 10 s and then freeze-thawed in liquid nitrogen twice. Samples were spun again, as described above, and supernatant was quantified with the bicinchoninic acid (BCA) assay and diluted with Tris-HCl–sucrose buffer.

DGL activity assay. Twenty-five-microgram tissue homogenates, in 0.1 ml of Tris-HCl–sucrose (pH 7.5), were incubated with 0.3 μM JZL184 (MGL inhibitor; Cayman Chemical, Ann Arbor, MI [58]) for 10 min at room temperature. Homogenates were incubated with 0.1 ml of solution of Tris-HCl with 0.2% Triton X-100 (pH 7.0) containing 20 nmol of dinonadecadienoin (Nu-Chek Prep, Waterville, MN; final volume, 0.2 ml/reaction) at 37°C for 30 min. The reaction was stopped by adding 1 ml of MeOH containing 25 pmol of $[^2H_5]$2-AG. Lipids were extracted as described above and analyzed via UPLC/MS/MS.

MGL activity assay. Ten-microgram tissue homogenates, in 0.1 ml of Tris-HCl–sucrose (pH 7.5), were incubated with 0.4 ml of solution of Tris-HCl with 0.1% bovine serum albumin (BSA; pH 8.0) containing 50 nmol of nonadecadienoin (Nu-Chek Prep; final volume, 0.5 ml/reaction) at 37°C for 10 min. The reaction was stopped by adding 1 ml of MeOH containing 10 nmol of heptadecanoic acid (Nu-Chek Prep). Lipids were extracted as described above and analyzed via UPLC/MS/MS.

Cytokine quantification. (i) ELISA. IL-5 quantification of intestinal homogenate and spleen supernatants was performed by standard sandwich enzyme-linked immunosorbent assay (ELISA) according to previously described protocols (56).

(ii) Cytokine bead array. IL-4, IFN-γ, and IL-10 quantification was performed on intestinal homogenate and supernatants from 72-h-stimulated splenocytes (5×10^6/well; 0.5 μg/ml of anti-CD3 and anti-CD28) using the Th1/Th2 CBA assay (BD Biosciences) according to the manufacturer's instructions.

RNA quantification. Mouse tissue recovered for RNA extraction was first incubated overnight in RNAlater (Qiagen) at 4°C and then extracted by TRIzol (Life Technologies). iScript reverse transcriptase (Bio-Rad) was used for cDNA synthesis. Real-time PCR was performed using iTaq Universal SYBR green Supermix (Bio-Rad) and the Bio-Rad CFX Connect. 18S primers were purchased from Qiagen, and *Cnr1* and *Cnr2* primers were purchased from Bio-Rad.

L3 infective juveniles (3 replicates of 500 to ~1,000) were collected from cultured rat fecal plates. L4 worms (3 replicates of 100 to 500) were collected from dissected lungs of infected rats 2 days postinfection. Adult worms (3 replicates of 100 to 200) were collected from dissected intestines of infected rats. Worms were washed in double-distilled water (ddH_2O), flash-frozen, and then homogenized in RiboZol (VWR) using pellet pestles and a pestle motor (Fisher Scientific and VWR). RNA was extracted according to RiboZol manufacturer instructions. Reverse transcription was done using ProtoScript II reverse transcriptase (New England BioLabs [NEB]), followed by real-time PCR as described above. Primer sequences were as follows: *N. brasiliensis* actin gene, ACGACGTGGCAGCTCTCGTTGTGG (forward) and GGTGCTTCGGTCAGCAGCACGGGA (reverse); *N. brasiliensis faah* gene, TCGGAGCAGGTGTTGTGAAGA (forward) and AGCCGGTACCACGGATCTGA (reverse); and *N. brasiliensis nape* gene, GGCGTACAGTCCAC GATGGTT (forward) and GGTGCTTCGGCTCGAGGTAG (reverse).

Gene orthology analysis and protein alignment. To identify enzymes and regulatory proteins involved in lipolysis and endocannabinoid signaling, we leveraged previously identified orthologs in *C. elegans* (31, 59). WormBase ParaSite (version WBPS9) was consulted to identify putative orthologs of these genes in several parasitic nematodes. To validate the putative parasitic nematode orthologs, we performed an orthology analysis using available predicted protein data sets from WormBase release WSPS: *Ancylostoma ceylanicum*, *Ancylostoma duodenale*, *Ascaris lumbricoides*, *Ascaris suum*, *C. elegans*, *Necator americanus*, *N. brasiliensis*, *Steinernema carpocapsae*, *Strongyloides ratti*, *Strongyloides stercoralis*, and *Toxocara canis*. Version 1.4 of the OrthoMCL pipeline was used to cluster proteins into families of

orthologous genes, with default settings and the BLAST parameters recommended in the OrthoMCL documentation (59).

The NAPE-PLD gene was further explored by aligning the sequences of mouse NAPE-PLD and the putative homolog from *N. brasiliensis*. Protein sequences were aligned using MUSCLE (60) and visualized using Mesquite (version 3.2). The accession numbers of the proteins used are NP_848843 for the mouse NAPE-PLD from GenBank and NBR_0001270801-mRNA-1 for the *N. brasiliensis* NAPE-PLD from WormBase ParaSite. The β-lactamase domain in the alignment was identified using the Smart protein database (61).

Gene expression analysis. To determine if genes for the endocannabinoid system are expressed in other parasitic nematodes, we downloaded the RNA-seq data for *T. canis* (62) (SRR1707010 and SRR1707031-6), *S. ratti* (63) (ERR299168-79 and ERR225783-4), *S. stercoralis* (64) (ERR146945-6 and ERR146948-9), *A. suum* (65) (SRR851186-95), *N. americanus* (66) (SRR609895 and SRR609951), *N. brasiliensis* (67) (PRJEB16076), and *A. ceylanicum* (68) (SRR1124912-4 and SRR1124985-6) from the NCBI database. The published RNA-seq data for *N. brasiliensis* were downloaded from the European Nucleotide Archive (http://www.ebi.ac.uk/). The reads were mapped to each species' indexed transcriptome (downloaded from WormBase ParaSite, WSPS9) with bowtie 1.0.0 in paired-end mode with the following settings: bowtie –X 800 -m 200 -S –seedlen 25 –trim3 [50 or 100] -n 2 –offrate 1 (69). Gene expression was quantified with RSEM version 1.2.31 (70).

Statistical analysis. GraphPad Prism software was used for statistical analyses. Where appropriate, Student's *t* test (for normal distribution data), one-way analysis of variance (ANOVA) (for analysis of more than two groups), two-way ANOVA (for analysis of more than one experiment), linear regression, and nonparametric Spearman correlation (for correlation analysis) were performed. Statistical significance is indicated in Table 1 and in figures as follows: *, $P \leq 0.05$; **, $P \leq 0.01$; and ***, $P \leq 0.0001$. To evaluate CB_1R inhibitor effect on *N. brasiliensis* burdens across experimental repeats, we employed linear mixed models. The inhibitor was tested as the main effect, which was adjusted by baseline weight and the weight on day 3; the experimental cooperation was the random effect. On the basis of the distribution types for egg and worm, the corresponding distribution families were Gamma and Poisson, respectively.

SUPPLEMENTAL MATERIAL

Supplemental material for this article may be found at https://doi.org/10.1128/IAI.00441-18.

SUPPLEMENTAL FILE 1, PDF file, 2.0 MB.

ACKNOWLEDGMENTS

These studies were supported by the NIH (grants 1R01AI091759-01A1 and R21AI137830 to M.G.N., R00DA034009 to N.V.D., K22AI119155 to A.R.D., and R21AI135500 to M.G.N., N.V.D., and A.R.D.) and initial complement from the UCR School of Medicine (to M.G.N. and N.V.D.).

We thank Spencer Wang, Sarah Bobardt, and Mark Barnes for assistance with the *Nippostrongylus brasiliensis* life cycle and assays.

M.G.N. and N.V.D. conceived and designed the experiments. H.M.B., J.C.J., D.A., D.L., J.K., and M.G.N. performed the experiments. J.C.J., D.A., H.M.B., N.V.D., D.L., S.G., and M.G.N. analyzed the data. M.M. and A.R.D. contributed bioinformatics analysis. M.G.N., N.V.D., and A.R.D. wrote the paper.

REFERENCES

1. Hotez PJ, Brindley PJ, Bethony JM, King CH, Pearce EJ, Jacobson J. 2008. Helminth infections: the great neglected tropical diseases. J Clin Invest 118:1311–1321. https://doi.org/10.1172/JCI34261.
2. Stephensen CB. 1999. Burden of infection on growth failure. J Nutr 129:534S–538S. https://doi.org/10.1093/jn/129.2.534S.
3. Shea-Donohue T, Qin B, Smith A. 2017. Parasites, nutrition, immune responses and biology of metabolic tissues. Parasite Immunol 39:e12422. https://doi.org/10.1111/pim.12422.
4. Ovington KS. 1986. Physiological responses of rats to primary infection with Nippostrongylus brasiliensis. J Helminthol 60:307–312. https://doi.org/10.1017/S0022149X00008543.
5. Wu D, Molofsky AB, Liang HE, Ricardo-Gonzalez RR, Jouihan HA, Bando JK, Chawla A, Locksley RM. 2011. Eosinophils sustain adipose alternatively activated macrophages associated with glucose homeostasis. Science 332:243–247. https://doi.org/10.1126/science.1201475.
6. Yang Z, Grinchuk V, Smith A, Qin B, Bohl JA, Sun R, Notari L, Zhang Z, Sesaki H, Urban JF, Shea-Donohue T, Zhao A. 2013. Parasitic nematode-induced modulation of body weight and associated metabolic dysfunction in mouse models of obesity. Infect Immun 81:1905–1914. https://doi.org/10.1128/IAI.00053-13.
7. Barnes MA, Carson MJ, Nair MG. 2015. Non-traditional cytokines: how catecholamines and adipokines influence macrophages in immunity, metabolism and the central nervous system. Cytokine 72:210–219. https://doi.org/10.1016/j.cyto.2015.01.008.
8. Howitt MR, Lavoie S, Michaud M, Blum AM, Tran SV, Weinstock JV, Gallini CA, Redding K, Margolskee RF, Osborne LC, Artis D, Garrett WS. 2016. Tuft cells, taste-chemosensory cells, orchestrate parasite type 2 immunity in the gut. Science 351:1329–1333. https://doi.org/10.1126/science.aaf1648.
9. DiPatrizio NV, Piomelli D. 2012. The thrifty lipids: endocannabinoids and the neural control of energy conservation. Trends Neurosci 35:403–411. https://doi.org/10.1016/j.tins.2012.04.006.
10. Simon V, Cota D. 2017. Mechanisms in endocrinology: endocannabinoids and metabolism: past, present and future. Eur J Endocrinol 176:R309–R324. https://doi.org/10.1530/EJE-16-1044.
11. Di Marzo V, Melck D, Bisogno T, De Petrocellis L. 1998. Endocannabinoids: endogenous cannabinoid receptor ligands with neuromodulatory action. Trends Neurosci 21:521–528. https://doi.org/10.1016/S0166-2236(98)01283-1.
12. Munro S, Thomas KL, Abu-Shaar M. 1993. Molecular characterization of

a peripheral receptor for cannabinoids. Nature 365:61–65. https://doi.org/10.1038/365061a0.
13. Galiègue S, Mary S, Marchand J, Dussossoy D, Carrière D, Carayon P, Bouaboula M, Shire D, Le Fur G, Casellas P. 1995. Expression of central and peripheral cannabinoid receptors in human immune tissues and leukocyte subpopulations. Eur J Biochem 232:54–61. https://doi.org/10.1111/j.1432-1033.1995.tb20780.x.
14. DiPatrizio NV, Igarashi M, Narayanaswami V, Murray C, Gancayco J, Russell A, Jung KM, Piomelli D. 2015. Fasting stimulates 2-AG biosynthesis in the small intestine: role of cholinergic pathways. Am J Physiol Regul Integr Comp Physiol 309:R805–R813. https://doi.org/10.1152/ajpregu.00239.2015.
15. DiPatrizio NV, Astarita G, Schwartz G, Li X, Piomelli D. 2011. Endocannabinoid signal in the gut controls dietary fat intake. Proc Natl Acad Sci U S A 108:12904–12908. https://doi.org/10.1073/pnas.1104675108.
16. Argueta DA, DiPatrizio NV. 2017. Peripheral endocannabinoid signaling controls hyperphagia in western diet-induced obesity. Physiol Behav 171:32–39. https://doi.org/10.1016/j.physbeh.2016.12.044.
17. Correa F, Hernangómez M, Mestre L, Loría F, Spagnolo A, Docagne F, Di Marzo V, Guaza C. 2010. Anandamide enhances IL-10 production in activated microglia by targeting CB(2) receptors: roles of ERK1/2, JNK, and NF-kappaB. Glia 58:135–147. https://doi.org/10.1002/glia.20907.
18. Nair MG, Herbert DR. 2016. Immune polarization by hookworms: taking cues from T helper type 2, type 2 innate lymphoid cells and alternatively activated macrophages. Immunology 148:115–124. https://doi.org/10.1111/imm.12601.
19. Storr MA, Keenan CM, Zhang H, Patel KD, Makriyannis A, Sharkey KA. 2009. Activation of the cannabinoid 2 receptor (CB2) protects against experimental colitis. Inflamm Bowel Dis 15:1678–1685. https://doi.org/10.1002/ibd.20960.
20. Turcotte C, Blanchet MR, Laviolette M, Flamand N. 2016. The CB2 receptor and its role as a regulator of inflammation. Cell Mol Life Sci 73:4449–4470. https://doi.org/10.1007/s00018-016-2300-4.
21. Bouchery T, Filbey K, Shepherd A, Chandler J, Patel D, Schmidt A, Camberis M, Peignier A, Smith AAT, Johnston K, Painter G, Pearson M, Giacomin P, Loukas A, Bottazzi ME, Hotez P, LeGros G. 2018. A novel blood-feeding detoxification pathway in Nippostrongylus brasiliensis L3 reveals a potential checkpoint for arresting hookworm development. PLoS Pathog 14:e1006931. https://doi.org/10.1371/journal.ppat.1006931.
22. Klein TW. 2005. Cannabinoid-based drugs as anti-inflammatory therapeutics. Nat Rev Immunol 5:400–411. https://doi.org/10.1038/nri1602.
23. Rodríguez de Fonseca F, Navarro M, Gómez R, Escuredo L, Nava F, Fu J, Murillo-Rodríguez E, Giuffrida A, LoVerme J, Gaetani S, Kathuria S, Gall C, Piomelli D. 2001. An anorexic lipid mediator regulated by feeding. Nature 414:209–212. https://doi.org/10.1038/35102582.
24. Randall PA, Vemuri VK, Segovia KN, Torres EF, Hosmer S, Nunes EJ, Santerre JL, Makriyannis A, Salamone JD. 2010. The novel cannabinoid CB1 antagonist AM6545 suppresses food intake and food-reinforced behavior. Pharmacol Biochem Behav 97:179–184. https://doi.org/10.1016/j.pbb.2010.07.021.
25. Tam J, Vemuri VK, Liu J, Bátkai S, Mukhopadhyay B, Godlewski G, Osei-Hyiaman D, Ohnuma S, Ambudkar SV, Pickel J, Makriyannis A, Kunos G. 2010. Peripheral CB1 cannabinoid receptor blockade improves cardiometabolic risk in mouse models of obesity. J Clin Invest 120:2953–2966. https://doi.org/10.1172/JCI42551.
26. Elphick MR. 2012. The evolution and comparative neurobiology of endocannabinoid signalling. Philos Trans R Soc Lond B Biol Sci 367:3201–3215. https://doi.org/10.1098/rstb.2011.0394.
27. Galles C, Prez GM, Penkov S, Boland S, Porta EOJ, Altabe SG, Labadie GR, Schmidt U, Knölker HJ, Kurzchalia TV, de Mendoza D. 2018. Endocannabinoids in Caenorhabditis elegans are essential for the mobilization of cholesterol from internal reserves. Sci Rep 8:6398. https://doi.org/10.1038/s41598-018-24925-8.
28. Savinainen JR, Saario SM, Laitinen JT. 2012. The serine hydrolases MAGL, ABHD6 and ABHD12 as guardians of 2-arachidonoylglycerol signalling through cannabinoid receptors. Acta Physiol (Oxf) 204:267–276. https://doi.org/10.1111/j.1748-1716.2011.02280.x.
29. Lehtonen M, Reisner K, Auriola S, Wong G, Callaway JC. 2008. Mass-spectrometric identification of anandamide and 2-arachidonoylglycerol in nematodes. Chem Biodivers 5:2431–2441. https://doi.org/10.1002/cbdv.200890208.
30. McPartland JM, Matias I, Di Marzo V, Glass M. 2006. Evolutionary origins of the endocannabinoid system. Gene 370:64–74. https://doi.org/10.1016/j.gene.2005.11.004.
31. Lucanic M, Held JM, Vantipalli MC, Klang IM, Graham JB, Gibson BW, Lithgow GJ, Gill MS. 2011. N-acylethanolamine signalling mediates the effect of diet on lifespan in Caenorhabditis elegans. Nature 473:226–229. https://doi.org/10.1038/nature10007.
32. Oakes MD, Law WJ, Clark T, Bamber BA, Komuniecki R. 2017. Cannabinoids activate monoaminergic signaling to modulate key C. elegans behaviors. J Neurosci 37:2859–2869. https://doi.org/10.1523/JNEUROSCI.3151-16.2017.
33. Reis Rodrigues P, Kaul TK, Ho JH, Lucanic M, Burkewitz K, Mair WB, Held JM, Bohn LM, Gill MS. 2016. Synthetic ligands of cannabinoid receptors affect Dauer formation in the nematode Caenorhabditis elegans. G3 (Bethesda) 6:1695–1705. https://doi.org/10.1534/g3.116.026997.
34. Howe KL, Bolt BJ, Shafie M, Kersey P, Berriman M. 2017. WormBase ParaSite—a comprehensive resource for helminth genomics. Mol Biochem Parasitol 215:2–10. https://doi.org/10.1016/j.molbiopara.2016.11.005.
35. Holroyd N, Sanchez-Flores A. 2012. Producing parasitic helminth reference and draft genomes at the Wellcome Trust Sanger Institute. Parasite Immunol 34:100–107. https://doi.org/10.1111/j.1365-3024.2011.01311.x.
36. Dotsey E, Ushach I, Pone E, Nakajima R, Jasinskas A, Argueta DA, Dillon A, DiPatrizio N, Davies H, Zlotnik A, Crompton PD, Felgner PL. 2017. Transient cannabinoid receptor 2 blockade during immunization heightens intensity and breadth of antigen-specific antibody responses in young and aged mice. Sci Rep 7:42584. https://doi.org/10.1038/srep42584.
37. Di Marzo V, Izzo AA. 2006. Endocannabinoid overactivity and intestinal inflammation. Gut 55:1373–1376. https://doi.org/10.1136/gut.2005.090472.
38. Katz D, Katz I, Porat-Katz BS, Shoenfeld Y. 2017. Medical cannabis: another piece in the mosaic of autoimmunity? Clin Pharmacol Ther 101:230–238. https://doi.org/10.1002/cpt.568.
39. Acharya N, Penukonda S, Shcheglova T, Hagymasi AT, Basu S, Srivastava PK. 2017. Endocannabinoid system acts as a regulator of immune homeostasis in the gut. Proc Natl Acad Sci U S A 114:5005–5010. https://doi.org/10.1073/pnas.1612177114.
40. Sykaras AG, Demenis C, Case RM, McLaughlin JT, Smith CP. 2012. Duodenal enteroendocrine I-cells contain mRNA transcripts encoding key endocannabinoid and fatty acid receptors. PLoS One 7:e42373. https://doi.org/10.1371/journal.pone.0042373.
41. Senin LL, Al-Massadi O, Folgueira C, Castelao C, Pardo M, Barja-Fernandez S, Roca-Rivada A, Amil M, Crujeiras AB, Garcia-Caballero T, Gabellieri E, Leis R, Dieguez C, Pagotto U, Casanueva FF, Seoane LM. 2013. The gastric CB1 receptor modulates ghrelin production through the mTOR pathway to regulate food intake. PLoS One 8:e80339. https://doi.org/10.1371/journal.pone.0080339.
42. Gay J, Ressayre L, Garcia-Villar R, Bueno L, Fioramonti J. 2003. Alteration of CCK-induced satiety in post-Nippostrongylus brasiliensis-infected rats. Brain Behav Immun 17:35–42. https://doi.org/10.1016/S0889-1591(02)00034-X.
43. Else KJ. 2005. Have gastrointestinal nematodes outwitted the immune system? Parasite Immunol 27:407–415. https://doi.org/10.1111/j.1365-3024.2005.00788.x.
44. Goumon Y, Casares F, Pryor S, Ferguson L, Brownawell B, Cadet P, Rialas CM, Welters ID, Sonetti D, Stefano GB. 2000. Ascaris suum, an intestinal parasite, produces morphine. J Immunol 165:339–343. https://doi.org/10.4049/jimmunol.165.1.339.
45. Golabi M, Naem S, Imani M, Dalirezh N. 2016. Evidence of morphine like substance and mu-opioid receptor expression in Toxacara canis (Nematoda: Ascaridae). Veterinary Research Forum 7:335–339.
46. Astarita G, Rourke BC, Andersen JB, Fu J, Kim JH, Bennett AF, Hicks JW, Piomelli D. 2006. Postprandial increase of oleoylethanolamide mobilization in small intestine of the Burmese python (Python molurus). Am J Physiol Regul Integr Comp Physiol 290:R1407–R1412. https://doi.org/10.1152/ajpregu.00664.2005.
47. Cottone E, Pomatto V, Cerri F, Campantico E, Mackie K, Delpero M, Guastalla A, Dati C, Bovolin P, Franzoni MF. 2013. Cannabinoid receptors are widely expressed in goldfish: molecular cloning of a CB2-like receptor and evaluation of CB1 and CB2 mRNA expression profiles in different organs. Fish Physiol Biochem 39:1287–1296. https://doi.org/10.1007/s10695-013-9783-9.
48. Pacioni G, Rapino C, Zarivi O, Falconi A, Leonardi M, Battista N, Colafarina S, Sergi M, Bonfigli A, Miranda M, Barsacchi D, Maccarrone M. 2015. Truffles contain endocannabinoid metabolic enzymes and anandamide. Phytochemistry 110:104–110. https://doi.org/10.1016/j.phytochem.2014.11.012.

49. Heng TS, Painter MW, Immunological Genome Project Consortium. 2008. The Immunological Genome Project: networks of gene expression in immune cells. Nat Immunol 9:1091–1094. https://doi.org/10.1038/ni1008-1091.
50. DiPatrizio NV. 2016. Endocannabinoids in the gut. Cannabis Cannabinoid Res 1:67–77. https://doi.org/10.1089/can.2016.0001.
51. Izzo AA, Sharkey KA. 2010. Cannabinoids and the gut: new developments and emerging concepts. Pharmacol Ther 126:21–38. https://doi.org/10.1016/j.pharmthera.2009.12.005.
52. Cani PD, Plovier H, Van Hul M, Geurts L, Delzenne NM, Druart C, Everard A. 2016. Endocannabinoids—at the crossroads between the gut microbiota and host metabolism. Nat Rev Endocrinol 12:133–143. https://doi.org/10.1038/nrendo.2015.211.
53. Goodridge HS, Marshall FA, Else KJ, Houston KM, Egan C, Al-Riyami L, Liew FY, Harnett W, Harnett MM. 2005. Immunomodulation via novel use of TLR4 by the filarial nematode phosphorylcholine-containing secreted product, ES-62. J Immunol 174:284–293. https://doi.org/10.4049/jimmunol.174.1.284.
54. Winter AD, Gillan V, Maitland K, Emes RD, Roberts B, McCormack G, Weir W, Protasio AV, Holroyd N, Berriman M, Britton C, Devaney E. 2015. A novel member of the let-7 microRNA family is associated with developmental transitions in filarial nematode parasites. BMC Genomics 16:331. https://doi.org/10.1186/s12864-015-1536-y.
55. Riner DK, Ferragine CE, Maynard SK, Davies SJ. 2013. Regulation of innate responses during pre-patent schistosome infection provides an immune environment permissive for parasite development. PLoS Pathog 9:e1003708. https://doi.org/10.1371/journal.ppat.1003708.
56. Chen G, Wang SH, Jang JC, Odegaard JI, Nair MG. 2016. Comparison of RELMalpha and RELMbeta single- and double-gene-deficient mice reveals that RELMalpha expression dictates inflammation and worm expulsion in hookworm infection. Infect Immun 84:1100–1111. https://doi.org/10.1128/IAI.01479-15.
57. Jang JC, Chen G, Wang SH, Barnes MA, Chung JI, Camberis M, Le Gros G, Cooper PJ, Steel C, Nutman TB, Lazar MA, Nair MG. 2015. Macrophage-derived human resistin is induced in multiple helminth infections and promotes inflammatory monocytes and increased parasite burden. PLoS Pathog 11:e1004579. https://doi.org/10.1371/journal.ppat.1004579.
58. Schlosburg JE, Blankman JL, Long JZ, Nomura DK, Pan B, Kinsey SG, Nguyen PT, Ramesh D, Booker L, Burston JJ, Thomas EA, Selley DE, Sim-Selley LJ, Liu QS, Lichtman AH, Cravatt BF. 2010. Chronic monoacylglycerol lipase blockade causes functional antagonism of the endocannabinoid system. Nat Neurosci 13:1113–1119. https://doi.org/10.1038/nn.2616.
59. Li L, Stoeckert CJ, Roos DS. 2003. OrthoMCL: identification of ortholog groups for eukaryotic genomes. Genome Res 13:2178–2189. https://doi.org/10.1101/gr.1224503.
60. Edgar RC. 2004. MUSCLE: multiple sequence alignment with high accuracy and high throughput. Nucleic Acids Res 32:1792–1797. https://doi.org/10.1093/nar/gkh340.
61. Letunic I, Doerks T, Bork P. 2015. SMART: recent updates, new developments and status in 2015. Nucleic Acids Res 43:D257–D260. https://doi.org/10.1093/nar/gku949.
62. Zhu XQ, Korhonen PK, Cai H, Young ND, Nejsum P, von Samson-Himmelstjerna G, Boag PR, Tan P, Li Q, Min J, Yang Y, Wang X, Fang X, Hall RS, Hofmann A, Sternberg PW, Jex AR, Gasser RB. 2015. Genetic blueprint of the zoonotic pathogen Toxocara canis. Nat Commun 6:6145. https://doi.org/10.1038/ncomms7145.
63. Hunt VL, Tsai IJ, Coghlan A, Reid AJ, Holroyd N, Foth BJ, Tracey A, Cotton JA, Stanley EJ, Beasley H, Bennett HM, Brooks K, Harsha B, Kajitani R, Kulkarni A, Harbecke D, Nagayasu E, Nichol S, Ogura Y, Quail MA, Randle N, Xia D, Brattig NW, Soblik H, Ribeiro DM, Sanchez-Flores A, Hayashi T, Itoh T, Denver DR, Grant W, Stoltzfus JD, Lok JB, Murayama H, Wastling J, Streit A, Kikuchi T, Viney M, Berriman M. 2016. The genomic basis of parasitism in the Strongyloides clade of nematodes. Nat Genet 48:299–307. https://doi.org/10.1038/ng.3495.
64. Stoltzfus JD, Minot S, Berriman M, Nolan TJ, Lok JB. 2012. RNAseq analysis of the parasitic nematode Strongyloides stercoralis reveals divergent regulation of canonical dauer pathways. PLoS Negl Trop Dis 6:e1854. https://doi.org/10.1371/journal.pntd.0001854.
65. Rosa BA, Jasmer DP, Mitreva M. 2014. Genome-wide tissue-specific gene expression, co-expression and regulation of co-expressed genes in adult nematode Ascaris suum. PLoS Negl Trop Dis 8:e2678. https://doi.org/10.1371/journal.pntd.0002678.
66. Tang YT, Gao X, Rosa BA, Abubucker S, Hallsworth-Pepin K, Martin J, Tyagi R, Heizer E, Zhang X, Bhonagiri-Palsikar V, Minx P, Warren WC, Wang Q, Zhan B, Hotez PJ, Sternberg PW, Dougall A, Gaze ST, Mulvenna J, Sotillo J, Ranganathan S, Rabelo EM, Wilson RW, Felgner PL, Bethony J, Hawdon JM, Gasser RB, Loukas A, Mitreva M. 2014. Genome of the human hookworm Necator americanus. Nat Genet 46:261–269. https://doi.org/10.1038/ng.2875.
67. Sotillo J, Sanchez-Flores A, Cantacessi C, Harcus Y, Pickering D, Bouchery T, Camberis M, Tang SC, Giacomin P, Mulvenna J, Mitreva M, Berriman M, LeGros G, Maizels RM, Loukas A. 2014. Secreted proteomes of different developmental stages of the gastrointestinal nematode Nippostrongylus brasiliensis. Mol Cell Proteomics 13:2736–2751. https://doi.org/10.1074/mcp.M114.038950.
68. Schwarz EM, Hu Y, Antoshechkin I, Miller MM, Sternberg PW, Aroian RV. 2015. The genome and transcriptome of the zoonotic hookworm Ancylostoma ceylanicum identify infection-specific gene families. Nat Genet 47:416–422. https://doi.org/10.1038/ng.3237.
69. Langmead B, Trapnell C, Pop M, Salzberg SL. 2009. Ultrafast and memory-efficient alignment of short DNA sequences to the human genome. Genome Biol 10:R25. https://doi.org/10.1186/gb-2009-10-3-r25.
70. Li B, Dewey CN. 2011. RSEM: accurate transcript quantification from RNA-Seq data with or without a reference genome. BMC Bioinformatics 12:323. https://doi.org/10.1186/1471-2105-12-323.
71. National Institutes of Health. 2015. Public Health Service policy on humane care and use of laboratory animals. Office of Laboratory Animal Welfare, National Institutes of Health, Bethesda, MD.